Antiviral activity of natural humic substances and shilajit materials against HIV-1: Relation to structure

Yury V. Zhernov [a], Andrey I. Konstantinov [b], Alexander Zherebker [c], Eugene Nikolaev [c], Alexey Orlov [c], Mikhail I. Savinykh [d], Galina V. Kornilaeva [e], Eduard V. Karamov [e], Irina V. Perminova [b],*

[a] National Research Center – Institute of Immunology FMBA of Russia, Moscow, 115522, Russia
[b] Lomonosov Moscow State University, Department of Chemistry, Moscow, 119991, Russia
[c] Skolkovo Institute of Science and Technology, Skolkovo, Moscow Region, 143026, Russia
[d] Scientific and Production Company "Sibdalmumiyo" Ltd., Novokuznetsk, Russia
[e] D.I. Ivanovsky Institute of Virology FSBI «National Research Center for Epidemiology and Microbiology Named After the Honorary Academician N.F. Gamaleya», Moscow, 123098, Russia

ARTICLE INFO

ABSTRACT

Natural products, such as humic substances (HS) and shilajit, are known to possess antiviral activity. Humic-like components are often called as carriers of biological activity of shilajit. The goal of this study was to evaluate anti-HIV activity of well characterized HS isolated from coal, peat, and peloids, and compare it to that of water-soluble organic matter (OM) isolated from different samples of Shilajit. The set of humic materials included 16 samples of different fractional composition: humic acid (HA), hymatomelanic acid (HMA), fulvic acid (FA). The set of shilajit OM included 19 samples of different geographic origin and level of alteration. The HIV-1 p24 antigen assay and cell viability test were used for assessment of antiviral activity. The HIV-1 Bru strain was used to infect CEM-SS cells. The obtained EC50 values varied from 0.37 to 1.4 mg L^{-1} for the humic materials, and from 14 to 142 mg L^{-1} for the shilajit OM. Hence, all humic materials used in this study outcompeted largely the shilajit materials with respect to anti-HIV activity: For the humic materials, the structure-activity relationships revealed strong correlation between the EC50 values and the content of aromatic carbon indicating the most important role of aromatic structures. For shilajit OM, the reverse relationship was obtained indicating the different mechanism of shilajit activity. The FTICRMS molecular assignments were used for ChEMBL data mining in search of the active humic molecules. As potential carriers of antiviral activity were identified aromatic structures with alkyl substituents, terpenoids, N-containing analogs of typical flavonoids, and aza-podophyllotoxins. The conclusion was made that the typical humic materials and Shilajit differ greatly in molecular composition, and the humic materials have substantial preferences as a natural source of antiviral agents as compared to shilajit.

1. Introduction

Fast evolution and mutation of viruses set forward a need for new antiviral agents suitable for treatment of drug-resistant infections. The multiple strains of the influenza viruses show resistance to adamantane derivatives (Dong et al., 2015), the herpes virus family – to acyclovir (Pottage et al., 1995), retroviruses – to azithromycin (Jeeninga et al., 2001). Due to a vast genetic diversity, the human immunodeficiency virus (HIV) develops quickly the resistance to monomolecular antiretroviral drugs (Karamov et al., 2018; Moskaleychik et al., 2015). Moreover, the pandemy of COVID-19, which hit already more than 5 million people globally, shows how limited a pool of antiviral drugs is (Dong et al., 2020; Ford et al., 2020; Li and De Clercq, 2020). In this respect, the natural supramolecular systems of biologically active compounds might be of particular value. Humic substances (HS) have been known for a long time for their antiviral activity (Helbig et al., 1997; Jooné et al., 2003; Klöcking et al., 2002). The different fractions of natural HS and synthetic HS-like materials are active against HIV (Botes et al., 2002; Brucolleri et al., 2013; Kornilaeva et al., 2019; Schneider

---

et al., 1996; Van Rensburg et al., 2002; Zhernov et al., 2017; Zhernov, 2018), influenza virus A/WSN/1933 (H1N1) (Lu et al., 2002), herpes simplex virus-1 (HSV-1) (Klöcking et al., 2002), Coxsackie virus A9 (Klöcking et al., 1972), tick-borne encephalitis virus (TBEV) (Orlov et al., 2019).

HS are the products of deep chemical and microbial oxidation of bioprecursors – lignins, tannins, peptides, cellulose, lipids, terpenoids, released from the remnants of plants and animals (Stevenson, 1994). These oxidized biomolecular precursors are assembled into supramolecular multicomponent systems of carboxyl and hydroxyl rich molecules. Given the presence of extended carbon backbone in these molecules, they can be considered as carboxylated polyanions (PAs). The latter have been intensively studied as components of microbicides aimed at prophylactics of viral infections (Zhernov and Khaitov, 2019; Zhan et al., 2016; Andrae-Marobela et al., 2013; Daglia, 2012). Shialit is another natural biologically active material, which is commonly used in traditional medicine (Agarwal et al., 2007). It is represented by brown to blackish-brown resinous matter found in the different mountain regions and considered to be a complex product of biotransformation of plant residues (Agarwal et al., 2007). Shilajit was reported as a dose-dependent inhibitor against HSV-1, HSV-2, human cytomegalovirus (HCMV), and respiratory syncytial virus (RSV) (Cagno et al., 2015). These are humic-like components, which are suggested to provide for multiple therapeutic properties of Shilajit (Schepetkin et al. 2003, 2009). However, the studies on direct comparison of the biological activity of HS from different sources (e.g., soil. peat, coal) and shilajit, as well as on the corresponding structure-activity relationships, are missing.

In our previous study on the anti-HIV activity of HS isolated from peloids (fresh water bottom sediments), we observed that the strongest inhibiting activity was characteristic of the most hydrophobic fractions of humic (HA) and hymatomelanic acids (HMA) (Zhernov et al., 2017). The most hydrophilic fraction of fulvic acid (FA) had the least activity. The structure-activity analysis revealed direct relationship between antiviral activity and the ratio of aromatic to aliphatic structures (lipophilicity index) of the different humic fractions used, and the inverse relationship with their carboxylic and total acidity. Given these previous results, we expanded largely the set of HS samples on the account of the most hydrophobic natural HS isolated from coal and peat. In addition, we included a broad set of crude shilajit samples to facilitate a direct comparison of biological activity of these two different natural products.

2. Materials and methods

2.1. Humic and shilajit materials used in this study

A set of humic and humic-like materials included 16 fractionated HS samples (HA, FA, HMA, as well as gray humic acid (CHG) from natural sources (coal, peat, peloid), one sample of oxidized lignin, and one sample of synthetic FA. Four samples of coal humic acids (CHA) were isolated by precipitation with acid followed by dialysis from the commercially available samples of potassium humates (Powhumus, Irkutsk Humate, Sakhalin Humate, Activated Humic Acid) and designated as (CHA-P), (CHA-I), (CHA-S), and CHA-A, respectively. One sample was isolated from lignite of the Baikal region (CHA-G) using alkali extraction (0.3 M NaOH). Peat HS included highmoor humic acid (PHA-T) and fulvic acid (PFA-5); lowmoor non-fractionated HS (PHF-1), and humic acid (PHA-1, PHA-3). Peloid humic materials were extracted from bottom sediments of the Molochka lake in Samara region and included humic acid (PelHA), fulvic acid (PelFA) and hymatomelanic acid (PelHMA). Peloid HS were extracted and fractionated according to the scheme described in our previous publication (Zhernov et al., 2017). The samples set also included veterinary pharmaceutical drug Ligfolum produced from the oxidized lignin, and a fulvic-like fraction of synthetic HS (MHQ-FA) synthesized via oxidative polymerization of phenols as described by (Zherebker et al., 2015). The latter represented a structural analogue of HS with the known molecular features.

Seventeen samples of raw shilajit materials originated from the different geographic regions (the Altai mountains in Russia and Mongolia, the Aldan river basin in Yakutia, Central Asia, the Caucasus). They were homogenised and dissolved in distilled water. Water extracts were centrifuged to separate insoluble part, and dried in a vacuum oven at temperature of 45 °C. This way 17 samples of shilajit mateials (SM) were prepared. The set of samples also included Altai "Golden mumiyo" (Sh-Alt, Russia) and Himalayan "Shilajit Dabur" (Sh-Him, India) pharmaceutical shilajit preparations.

The full set of humic and shilajit materials used in this study, along with their CHNO elemental compositions are listed in Table S1 in Supplementary Material.

2.2. Structural characterization of the HS and shilajit materials

^{13}C NMR spectra were acquired using a Bruker Avance 400 NMR spectrometer operating at 400 MHz proton frequency. All humic and shilajit solutions were prepared as following: a weight of 45 mg of a sample was dissolved in 0.6 mL of 0.3M NaOD/D2O with isotope purity of 99+% (Aldrich). For suppressing the nuclear Overhauser effect, the broadband decoupling from protons was switched off for the relaxation delay time. The relaxation time delay was 7.8 s in accordance with the conditions described by (Kovalevski et al., 2000). The NMR assignments were made after (Hertkorn et al., 2002): carbon of alkyl chains (CHn) – 0–50 ppm; carbon of alkoxide groups CH_3O – 50–58 ppm, CH_2O – 58–65 ppm, CHO – 65–90 ppm, and OCO – 90–110 ppm; aromatic carbon bonded with H or C atoms (Car) – 110–145 ppm; aromatic carbon

bonded with oxygen (CarO) – 145–165 ppm; carbon of carboxylic groups (COO) – 165–187 ppm; carbon of carbonyl groups (C═O) – 187–220 ppm. In case of shilajit samples characterized with significant content of nitrogen (see Table S3 in Supplementary Material), the spectral intervals of 50–65 and 165–187 ppm were also attributed, respectively, to CH–N groups of amino acids and to amide structures (CO–N).

2.3. Compilation of the FTICR MS data set for the HS and shilajit materials

For characterization of molecular space of the set of HS samples used in this study the previously published FTICR mass-spectrometric data (peak lists) were used for CHA-G, CHA-P, CHA-S, PelHA, PelHMA, PekFA, PHA-5, PFA-5, MHQ-FA were used (Orlov et al., 2019; Zhernov et al., 2017). Mass-spectrum of the Shelajit sample Sh1 was obtained using 7T FTICR MS Apex Ultra (Bruker Daltonics, Germaby) equipped with the harmonized cell (Nikolaev et al., 2011) and electrospray ionization (ESI) source operating in negative ion mode. The spectra were acquired with a time domain of 4 megawords in ESI (−) and 300 scans were accumulated for each spectrum. Resolving power was 530 000 at m/z = 400. Here all spectra were first externally calibrated using the synthesized carboxylated polystyrene as described previously (Zherebker et al., 2017), followed by internal calibration using fatty acids residual signals (Sleighter et al., 2008) which yielded accuracy values < 0.5 ppm. Only peaks with a signal to noise (S/N) ratio exceeding 6 were used for formulae assignment.

Molecular compositions were assigned using the open source browser-based application UltraMassExplorer created by Leefmann et al. (http://dockersrv1.awi.de:3838/ume) (Leefmann et al., 2019). The pivot table with all assigned formulae is presented in Supplementary file Table S5. The generated CHONS formulas were validated by setting sensible chemical constraints typical for DOM (O/C ratio ≤ 1, 0.3<H/C ratio ≤ 2.2, element counts (C ≤ 120, H ≤ 200, 0<O ≤ 60, N ≤ 2, S ≤ 1) and mass accuracy window < 0.5 ppm) (Kunenkov et al., 2009; Sleighter et al., 2007). Additionally, for HS only formulae presenting in at least two samples were considered. All formulae were further divided into three categories according to a modified aromaticity index (AI_{mod}) proposed by (Koch et al., 2016) AI_{mod} was calculated according to the following equation (1):

$$AI_{mod} = \frac{1 + C - 0.5O - S - 0.5(N + H)}{C - 0.5O - N - S} \qquad (1)$$

where C, H, O, N, S are the numbers of atoms in molecular formulae.

2.4. HIV-1 p24 antigen assay and cell viability test

The HIV-1 Bru strain was used in this study to infect CEM-SS cells which were derived from the human lymphoblastoid cell line CEM that expresses high levels of the CD4 antigen (Wain-Hobson et al., 1991). The cells were cultured in the suspension medium RPMI-1640 (Gibco) containing 10% FCS. The CEM-SS cells were cultured at a density of 7.0×10^4/well and infected with HIV_{BRU} at the multiplicity of infection (MOI) of 1. All solutions of the HS and shilajit samples were sterilized using 0.22 μm syringe-filters (Merck Millipore Ltd) and stored at −20 °C until use. CEM-SS cells were incubated for 24 h in the absence and presence of HS and SM samples in 96-well plates. The HS and shilajit samples were homogeneous and stable throughout the incubation period in a 96-well plate. As a control, we used the reference HIV-1 inhibitors: the reverse transcriptase inhibitor Azidothymidine (AZT) and the integrase inhibitor Raltegravir (RAL). They were purchased from Sigma-Aldrich. After 3 days following three washings, CEM-SS cells were cultured in 96 well plates for 3 days to measure p24 release. The level of virus replication was detected by ELISA using a «HIV-1 p24 antigen-ELISA-BEST » test system (Vector-Best, Novosibirsk, Russia). The effects on cell viability

were monitored by MTT (3-(4,5-dimethylthiazol-2-yl)-2,5-diphenyl tetrazolium bromide) assay, which measures the reduction of yellow MTT to purple formazan by mitochondrial enzymes (Mosmann, 1983).

2.5. Statistical analyses

EC50 and CC50 values were calculated using GraphPad Prism v.5.00 software (GraphPad Software, La Jolla, CA). The approximation for sigmoidal dose-response was used with variable slope by setting the following constraints: fixed top of 100, and fixed bottom of 0. As internal acceptance criteria, R^2 values were set to ≥0.9. The therapeutic value of the drug was estimated using the selectivity index (SI). It is calculated as a ratio of 50% cytotoxic concentration (CC50) to 50% effective concentration (EC50). Statistical significance was determined using one-way Anova with the Bonferroni *post hoc test* (p < 0.0001).

2.6. ChEMBL data mining and analysis

ChEMBL data retrieval was performed similarly to the previously developed pipeline (Orlov et al., 2019; Fedoros et al., 2018). MySQL edition of ChEMBL26 was used for data mining. Briefly, ChEMBL dump file was put into a local MySQL database. All *molregno* and *canonical_smiles* entries were extracted from *compound_structures* table. Entries of *canonical_smiles* field containing disconnected fragments (entries containing "." symbol) were additionally preprocessed in the following way. All entries were split at '.' symbol and the largest SMILES substring was kept. Compounds corresponding to these SMILES were further neutralized using RDKit (RDKit: Open-source chemoinformatics; http://www.rdkit.org). rdMolStandardize module and formulae for all found compounds were generated using RDKit. Then the formulae of the samples with the Spearman rank correlation coefficient with EC50 lower or equal to −0.7 (339 formulae) were searched among all formulae from the ChEMBL data base. The data on compound structures (*compound_structures*), activities (*activities*), bioassays (*assays*), etc. were extracted from ChEMBL. To retrieve the activity entries relevant to HIV, case insensitive substring query searching using 'HIV' and 'human immunodeficiency' strings was performed in *assays.description* and *assays. organism*, *assays.mc_organism* fields. All extracted entries were manually analyzed.Network-based representation was constructed using Data-Warrior (v.5.2.1) software (Sander et al., 2015). Stereo-depleted SMILES strings were used for the calculation of DataWarrior's FragFP fingerprints and network building. Tanimoto index cut-off was set to 0.8. Thus, each network node corresponds to the structure (with removed stereochemistry information) and edge corresponds to structural similarity index above cut-off.

3. Results and discussion

3.1. Antiviral activity and cytotoxicity of the humic and shilajit materials used in this study

The cytotoxicity of the humic and shilajit samples with respect to the CEM-SS cells was assessed using MTT assay. For the majority of the humic and shilajit samples at a concentration of 1000 mg L^{-1}, the mitochondrial activity was above 80%. Ligfolum exhibited low toxicity (CC50 = 708 mg L^{-1}). The FA samples under study at a concentration of 1000 mg L^{-1} also caused a decrease in mitochondrial activity below 80%, but it was still above 70%. The obtained results are indicative of good safety profile both for humic and shilajit materials used in this study.

The typical dose-inhibition curves against HIV-1 infection for the humic and shilajit materials of different origin and/or fractional composition are shown in Fig. 1. The full set of the EC50 values obtained for the humic and Shilajit samples used in this study is summarized in Table 1. It can be seen that the humic materials were characterized with much higher inhibitory activity with respect to HIV-1 replication in
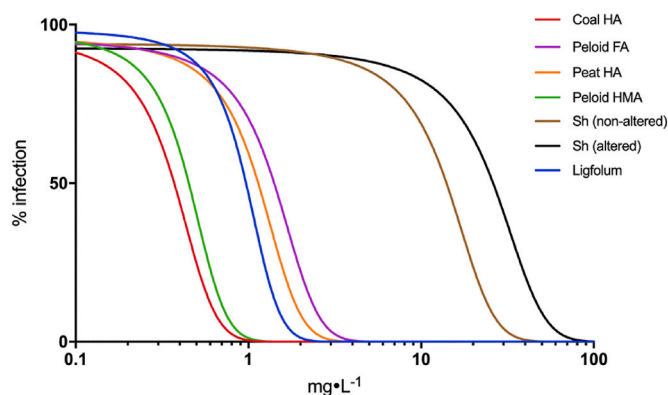
Fig. 1. The typical dose-inhibition curves for the humic and shilajit materials from different sources and/or fractional composition (n = 3; $R^2 > 0.9$). The samples are highlighted as follows: coal HA (red), peloid FA (violet), peat HA (orange), peloid HMA (green), non-altered Sh (black), altered Sh (brown), Ligfolum (blue). (For interpretation of the references to color in this figure legend, the reader is referred to the Web version of this article.)

CEM-SS cells as compared to the water extracts of Shilajit samples used in this study. The EC50 values of humic materials (Table 1) ranged from 0.37 to 1.41 mg L^{-1}, whereas for the of shilajit samples they did not exceed 14 mg·L^{-1}.

The highest activity was observed for the most hydrophobic and aromatic enriched coal humic acids. The comparable activity was characteristic for the peloid humic acids and hymatomelanic acid. Peat HA had intermediary activity, and the lowest activity was observed for low molecular weight oxidized FA is significantly lower. At the same time all Shilajit samples had the least activity. The altered shilajit samples were characterized with the higher activity as compared to the non-altered ones.

The EC50 values measured for coal and peloid HA and HMA ranged from 0.37 to 0.72 mg L^{-1} outcompeting the oxidized lignin sample Ligfolum (0.96 ± 0.11 mg L^{-1}). The reference HIV-1 inhibitors predictably showed better activity than the HS samples used in this study: The EC50 values determined for AZT and RAL were 5.5 and 3.4 ng L^{-1}, respectively. Some of the EC50 values found for coal and peloid HA were even lower than the best reported values for the synthetic carboxylated polyanions (PA) (0.76–0.97 mg L^{-1}) (Leydet et al., 1998; Savage et al., 2014; Schols et al., 1991) indicating high activity of the humic materials

used in this study, which can be treated as humic PAs. The EC50 value of the highmoor peat HA (PHA-5) (0.79 mg L^{-1}) was close to coal HA, whereas the corresponding values for the lowmoor HA and non-fractionated HS were in the range from 1.13 to 1.22 mg L^{-1}. The EC50 values of all FA samples ranged from 1.26 to 1.41 mg L^{-1}. The similar activity had the synthetic FA (MHQ-FA) (1.27 mg L^{-1}). It should be noted that this synthetic FA was obtained by oxidative polycondensation of hydroquinone with model phenylpropanoic acid (Zherebker et al., 2015). It was enriched with aliphatic, carboxyl and OCO fragments despite the aromatic nature of the monomers. The carbon distribution in this sample was characteristic of fulvic acids, for example, PFA. This might be indicative of lower activity of more oxidized, hydrophilic, low molecular weight humic materials (e.g., FA fractions) as compared to more hydrophobic, enriched with aromatic structures humic materials (e.g., HA, HMA, gray HA fractions).

For better visualization of the differences in anti-HIV properties between humic and Shilajit materials, we plotted all EC50 values and selectivity index (SI) values in Fig. 2. The clustering of shilajit materials is visible in Fig. 2B: three groups of shilajit materials can be distinguished with similar activity within the cluster (each cluster is marked with different colors). All 19 shilajit samples used in this study were characterized with two orders of magnitude lower anti-HIV activity as compared to the humic materials (Fig. 2B, Table 1). The EC50 values measured for the shilajit samples ranged from 14 to 142 mg L^{-1}. The selectivity index (SI) for all studied samples of the shilajit (except for Sh29 sample) did not exceed 10. Even the EC50 values of the least active samples of FA were an order of magnitude lower (the activity higher) as compared to the most active sample of shilajit. Still, there was substantial variation observed within the shilajit samples. The highest activity was observed in the black, least altered samples of shilajit, while the least activity was observed in the weathered (brownish to yellowish samples of shilajit).

3.2. Structure-antiviral activity relationships derived from ^{13}C NMR data on the humic and shilajit materials used in this study

In order to reveal the relationship between anti-HIV activity and structural features of the humic and shilajit materials used in this study, their structural composition was determined with a use of quantitative solution-state ^{13}C NMR spectroscopy. The ^{13}C NMR spectra of the HS samples under study were typical of HS represented by broad, highly overlapped signals (Fig. 3a,b).

Table 1
The antiviral activity of the humic and shilajit materials used in this study.

Humic samples	Source	EC50 (mg·L^{-1})[a]	Shilajit samples	Description	EC50 (mg·L^{-1})[c]
CHA-G	Coal	0.37 ± 0.03	Sh1	Black and rust-colored, altered, Altai	97.69 ± 0.44
CHA-S	Coal	0.43 ± 0.03	Sh3	Black and rust-colored, altered, Aldan	54.63 ± 0.64
CHG-P	Coal	0.53 ± 0.05	Sh4	Blackish-brown, altered, Altai	103.2 ± 0.2
CHA-P	Coal	0.53 ± 0.03	Sh6	Blackish-brown, altered, Altai	99.23 ± 0.29
CHA-A	Coal	0.69 ± 0.06	Sh7	Brown, altered, Altai	104.2 ± 0.21
CHA-I	Coal	0.72 ± 0.04	Sh9	Black, low altered, Altai	48.84 ± 0.41
PelHMA	Peloid	0.45 ± 0.06	Sh13	Blackish-brown, altered, Altai	38.78 ± 0.4
PelHA	Peloid	0.58 ± 0.02	Sh15	Yellow-brown, altered, Pamir	96.95 ± 0.64
PelHFA	Peloid	1.00 ± 0.06	Sh18	Blackish-brown, altered, Altai	60.81 ± 0.44
Ligfolum	Oxidized lignin	0.96 ± 0.11	Sh19	Blackish-brown, altered, Central Asia	26.13 ± 0.21
PHA-5	Peat	0.80 ± 0.03	Sh20	Blackish-brown, altered, Altai	98.85 ± 0.41
PHF-1	Peat	1.13 ± 0.03	Sh22	Blackish-brown, altered, Altai	40.1 ± 0.48
PHF-3	Peat	1.14 ± 0.03	Sh25	Black, low altered, Altai	110.1 ± 0.32
PHA-1	Peat	1.20 ± 0.04	Sh29	Black, low altered, Afganistan	14.03 ± 0.62
PHA-3	Peat	1.22 ± 0.03	Sh30	Black, low altered, Afganistan	54.12 ± 0.36
Fulvic samples	**Source**	**EC50 (mg·L^{-1})[b]**	Sh32	Black, altered, Caucasus	90.6 ± 0.67
PFA-5	Peat	1.27 ± 0.01	Sh38	Black, low altered, Altai	81.06 ± 0.41
MHQ-FA	Synthetic FA	1.27 ± 0.02	Sh-Alt	Pharmaceutical drug, Altai	44.74 ± 0.22
PelFA	Peloid	1.41 ± 0.04	Sh-Him	Pharmaceutical drug, Himalayas	48.0 ± 0.1

[a] M±SD, n = 3 (CC50 > 1000 mg L^{-1} for all studied humic acid samples).

[b] M±SD, n = 3 (CC50 > 500 mg L^{-1} for all studied fulvic acid samples).

[c] M±SD, n = 3 (CC50 > 200 mg L^{-1} for all studied shilajit samples).
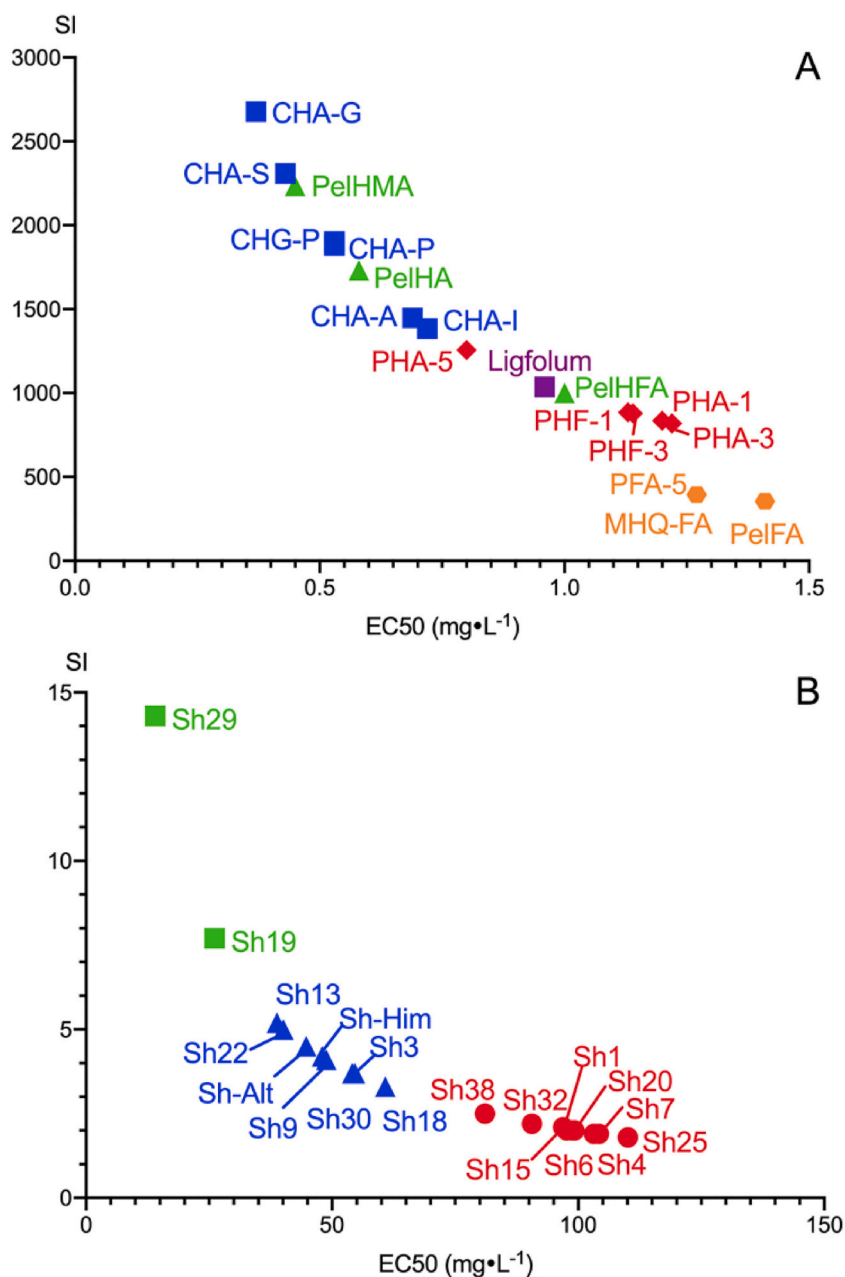
Fig. 2. The humic (A) and shilajit (B) materials clustering based on SI and EC50: (A) blue squares – HA from coal; green triangles – HA, HMA and HFA from peloid, red rhombuses – HA and HFA from peat, purple square – oxidized lignin, orange hexagon – FA of various sources of origin. (B) Green, red, and blue colors are shown separating different array clusters of shilajit samples. (For interpretation of the references to color in this figure legend, the reader is referred to the Web version of this article.)

The coal HA were characterized with the presence of intense spectral band in the range of aromatic carbon (110–165 ppm), signals of alkyl chains (0–50 ppm), and carboxylic groups (165–185 ppm). The minimum intensity was observed in the range of alkoxide (predominantly, carbohydrate) structures (50–100 ppm). The peat FA were characterized with the presence of an intense signal in the range of carbohydrate structures (60–90 ppm), aromatic and carboxylic groups. The aromatic region was characterized with three distinct peaks at 115, 130 and 156 ppm: the first and second ones are characteristic of aromatic carbon in *o*- and *p*-position to hydroxy groups, the third one corresponds to Car-O carbon indicating high degree of oxidation of FA and its enrichment with OH- and COOH- groups.

^{13}C NMR spectra of shilajit are very different from the HA-related materials (Fig. 3c). The spectra are characterized with the presence of a broad band of alkyl chains (0–50 ppm), sharp signals of carbohydrate and primary/secondary amine structures (65–90 ppm), and carboxylic groups (165–185 ppm). A distinct group of sharp peaks at 127–135 ppm, which were characteristic of all spectra of shilajit, was attributed to

aromatic carbon of hippuric acid. The latter is a typical component of shilajit (Agarwal et al., 2007; Konstantinov et al., 2013). A sharp signal at 165 ppm was attributed to amide structures of peptide chains and hippuric acid. Despite the striking difference to coal HA, the ^{13}C NMR spectra of shilajit were rather similar to the spectra of peat FA (Fig. 2b, c). Given that this study used water-extractable portion of shilajit organic matter, it should have much more in common with the acid-soluble fraction of HS - fulvic acid - as compared to the acid-insoluble humic acid. Fulvic acid is characterized with the highest contribution of oxygen-containing functions, which has some similarity with the organic matter of water-soluble fraction of shilajit.

Quantitative structural data for each sample were obtained as a set of integrals of ^{13}C NMR spectral regions assigned to typical structural units of humic and shilajit materials. They are given in Table S2 in the SI. The highest content of aromatic carbon (Car and CarO) (from 51 to 61% of the total C) was characteristic of humic acids and their fractions isolated from coal and peloid. These samples were characterized with the lowest content of carbohydrate moieties and methoxyl groups (4–15%). On
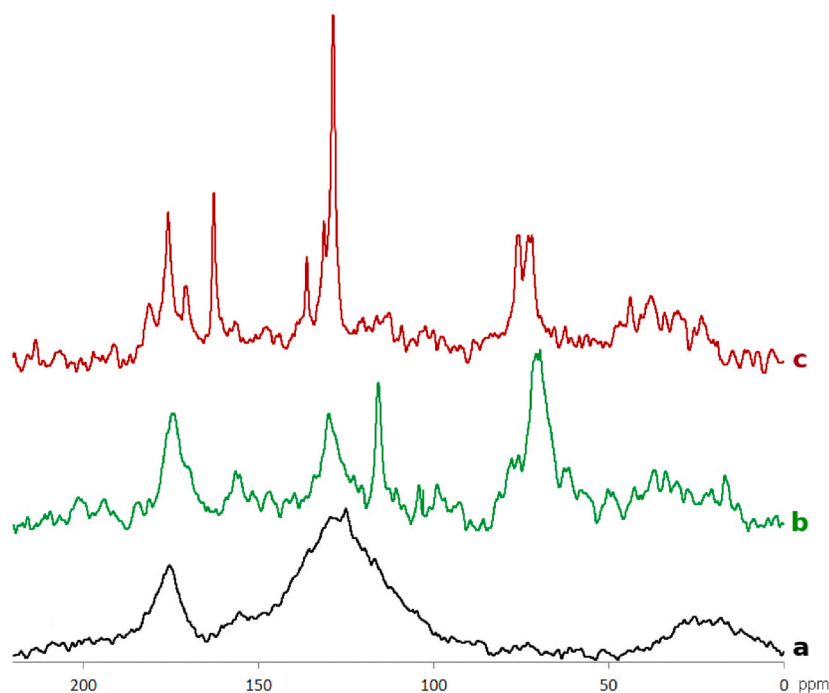
Fig. 3. Typical ^{13}C NMR spectra of coal humic acids (a), peat fulvic acids (b), and shilajit (c).

contrary, the peat humic materials and all fulvic acids used in this study were characterized with the lower content of aromatic carbon (34–39%) and much higher content of carbohydrate moieties (from 23 to 34%). The content of alkyl carbon (CHn) and carboxylic (COO) structures varied from 8 to 21% and 9–18%, respectively (see Table S3 in Supplementary Material). The shilajit samples under study were characterized with contribution of total aromatic and alkoxide (along with amino acid) structures in the range of 24–38% and 22–33%, respectively, that was similar to those measured for fulvic acids of peat. The content of alkylic and carboxylic/amide carbon ranged from 18 to 31% and from 8 to 15%, respectively (see Table S3 in Supplementary Material).

The discussed above quantitative data on structural group composition of the humic and shilajit samples were used for correlation analysis with the set of the corresponding data on antiviral activity. The obtained data are shown in Fig. 4A and B and Figs. S1 and S2 in Supplementary Material. It can be seen that the EC50 values of the humic materials used in this study were inversely related to the content of unsubstituted aromatic carbon (Car) ($r = -0,84$; $p = 0.00095$) (Fig. 4A).

A significant positive relationship was observed for the content of CH_2O groups ($r = 0.7$; $p = 0.004$). This might be indicative of a drop in activity of the HS samples with increasing content of carbohydrates. The correlation analysis for the shilajit samples yielded the opposite trends. The strongest inverse relationship was observed with the content of CH_3O & CH_2O or CH–N ($r = -0.63$; $p = 0.004$). On contrary to HS, antiviral activity of shilajit was inversely related to the content of aromatic structures reflected in the positive correlation between EC50 and Car ($r = 0.61$; $p = 0.006$) (Fig. 4B). This might be indicative of the different mechanism of activity inherent within shilajit materials as compared to humic acid-dominated humic materials, e.g. coal, peat, peloids, etc. Given the substantial impact of structural group composition of both humic and shilajit samples on their antiviral activity, it was of particular interest to search for the relationships between molecular composition of HS and shilajit and their antiviral activity. The information on molecular composition is provided by FTICR MS. In this study, we had at our disposal FTICR MS data only for the subset of humic materials. This is a reason why we could conduct the respective studies only on the humic materials.

3.3. Structure-antiviral activity relationships derived for the FTICR MS data on the HS samples used in this study

For depiction of molecular composition of humic materials, we used FTICR MS data on nine (out of 16) HS samples used in this study. The amount of empirical formulae, which were present in, at least, 2 samples, ranged from 1902 to 4400. Van Krevelen diagrams for the respective HS samples are shown in Fig. 5. One available spectrum of the shilajit sample (Sh1) is given for comparison.

The dots in Van Krevelen diagrams are highlighted in different colors with respect to the value of aromaticity index (AI_{mod}). The latter is introduced to evaluate aromaticity of molecular components of complex mixtures (Koch et al., 2006): the values of $AI_{mod} \geq 0.67$ and > 0.5 correspond to condensed aromatic and aromatic compounds, respectively. This representation reveals drastic difference in molecular composition of the samples used in this study: the humic acid samples from coal, peloid, and peat are dominated by condensed and aromatic compounds, whereas the fulvic acid samples (and shilajit) are characterized by maximum contribution of highly oxidized unsaturated and saturated compounds with AI below 0.5. These data corroborate well the FTICR MS results reported by Khanna et al. (2008): the authors found very similar molecular space for fulvic acids extracted from Shilajit, which was located above AI = 0.5 line. This characterizes shilajit as very hydrophilic material dominated with carbohydrates and nitrogen-containing compounds. High content of nitrogen (up to 14%) is a remarkable feature of shilajit materials which is very different from N-depleted humic materials (up to 4%) as follows from comparison of the elemental compositions of the sample sets (Table S1).

Of importance is that the first group of samples (all humic acids) is characterized with high anti-HIV activity, whereas the second group (all fulvic acids including shilajit) are characterized with low anti-HIV activity. For revealing molecular composition – anti HIV relationship, the relative intensities of the corresponding peaks in mass-spectra (Supplementary Info Table S5) were used for calculation of Spearman rank correlation with EC_{50}. For better visualization, the data were plotted in van Krevelen diagram with color-coded correlation of molecular constituents (Fig. 6).

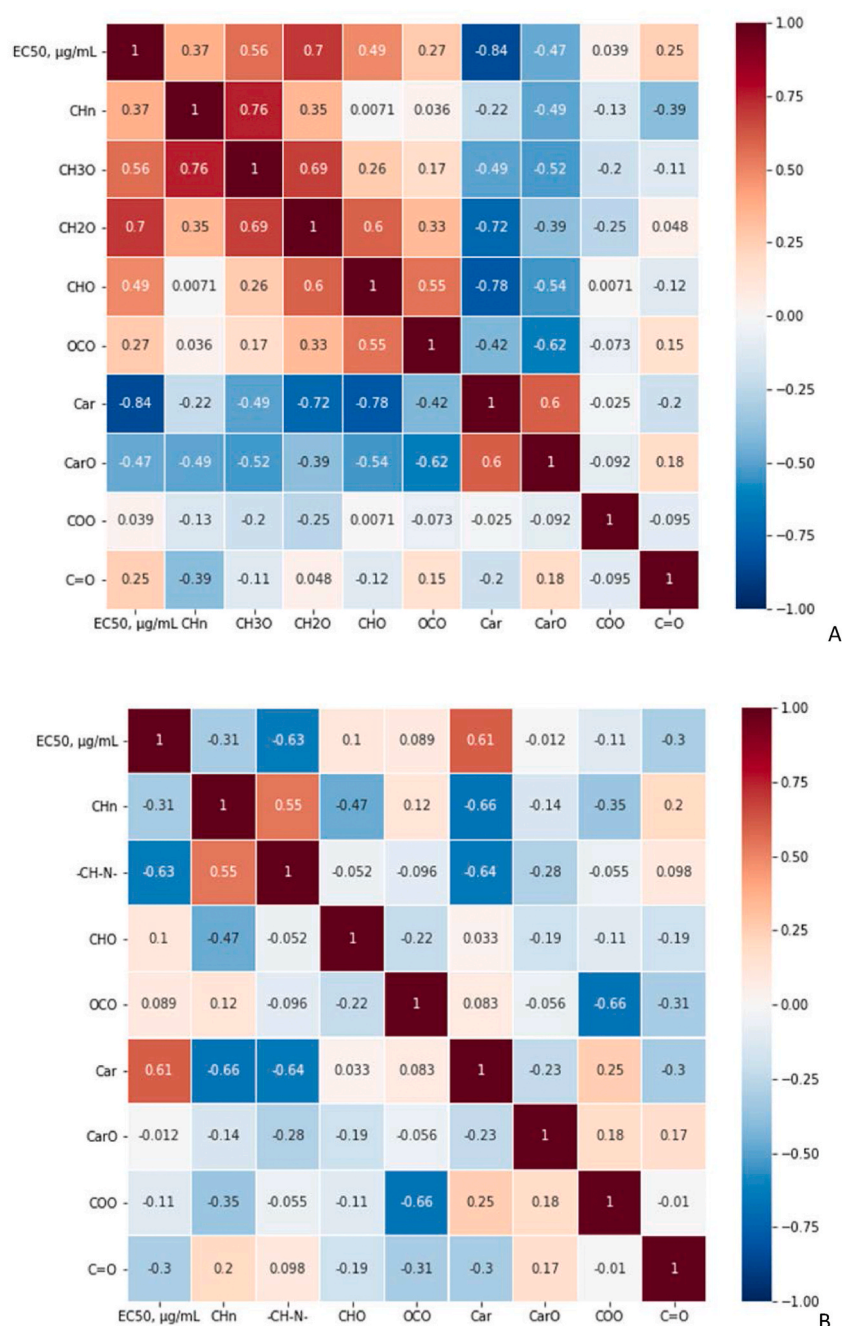It was found that 339 and 201 formulae possessed strong negative

Fig. 4. The matrix of Spearman correlation coefficients for the EC50 values and the content of carbon in the different chemical environments as measured by ^{13}C NMR spectroscopy: A) for the humic materials used in this study (n = 15); B) for the shilajit materials (n = 19).

and positive correlation ($|r| > 0.7$ with $p < 0.05$) with EC$_{50}$, respectively. Of interest is that 251 out of 339 molecular components with the strong negative correlation of EC50 were CHNO compositions. It can be deduced that the inhibitory activity is mostly related to the presence of relatively reduced aromatic compounds with H/C < 1 and O/C < 0.5. This is in agreement with the close correlation between the content of aromatic moieties and EC50 as it was revealed by the NMR data.

In search of potential structural candidates for the most active components in the humic molecular ensemble, we have mined the data for 339 highly correlated formulae (Spearman's rank correlation coefficient ≤ -0.7) in ChEMBL database. We found 792 structures and 7271 activity entries corresponding to the 112 formulae (Supplementary Info Tables S7) and 642 out of which contained N atom and 65 – S atom. The assays entries (55) and the corresponding activity entries (76) related to

anti-HIV activity measurement were also retrieved (Supplementary file Table S6). Almost half of the assays included inhibition of the specific HIV protein (mostly, integrase), while the other half was presented by the assessment of antiviral activity in the cell-based assays. Several examples of the retrieved active structures, which are the derivatives of naturally occurring compounds, and corresponding activities, are presented in Table 2. The full data are shown in Table S6 in the Supplementary Material.

Molecular formulae may correspond to a number of isomers. That is why the structural space of the active components is significantly broader as compared to molecular composition space. For deeper analysis of structures suggested for the HS components, the molecular network was plotted. ChEMBL data mining showed the presence of distinct clusters on the structural space network (Fig. 7). These clusters
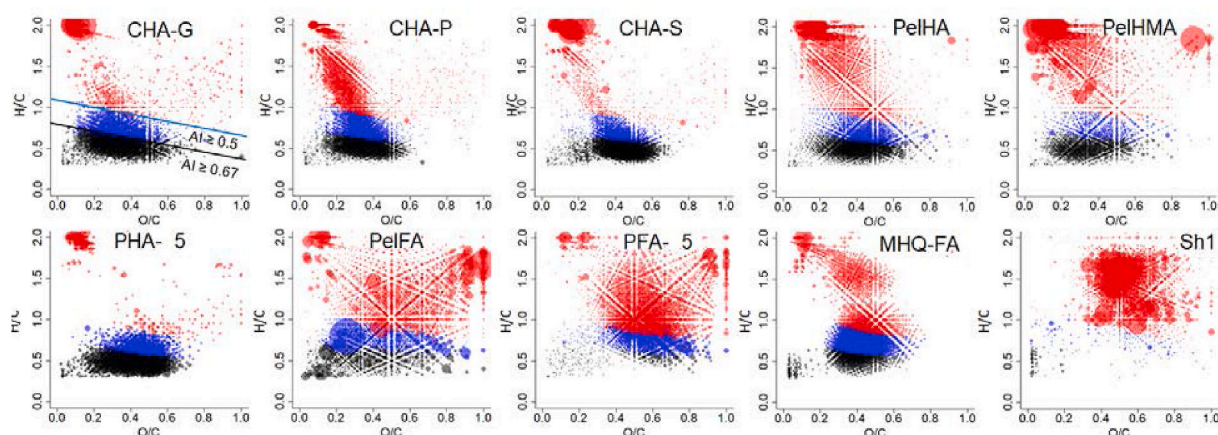
Fig. 5. Van Krevelen diagrams constructed on FTICR MS data of the 9 humic materials and 1 shilajit sample under study. Colors correspond to aromaticity of molecules: black – condensed aromatics ($AI_{mod} \geq 0{,}67$); blue – aromatics ($AI_{mod} \geq 0{,}5$); red – non-aromatics ($AI_{mod} < 0{,}5$). (For interpretation of the references to color in this figure legend, the reader is referred to the Web version of this article.)
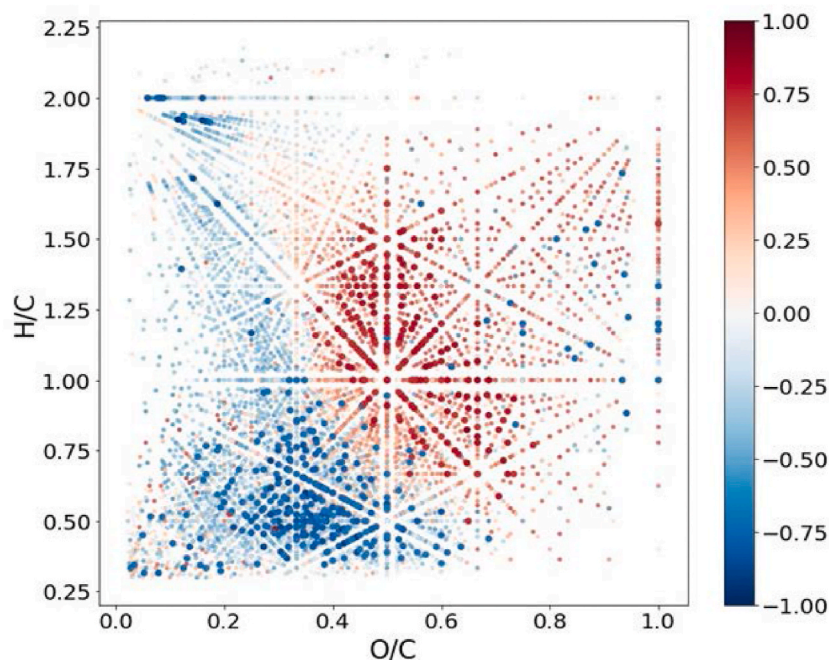

Fig. 6. Van Krevelen diagram for all formulae present in the set of 9 HS sample under study with color-coded Spearman correlation coefficient with EC50 values. (For interpretation of the references to color in this figure legend, the reader is referred to the Web version of this article.)
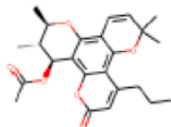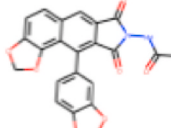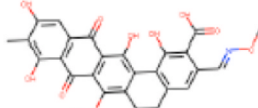
are produced by the structures with high chemical similarity – with the values of fingerprints T-score exceeding 0.8. In the most cases, the formulae assigned with the similar structures had the similar relationship to the EC50 values.

The largest cluster (19 nodes) is related to ether derivatives of 4′-O-demethylepipodophyllotoxins active against human DNA topoisomerase II (Zhou et al., 1991). Among the other largest clusters produced by the formulae, which are highly correlated to activity of the HS samples, there is the cluster of terpenoids from the Rhizome of *Alisma orientale*, tested against human Human Carboxylesterase 2 (Mai et al., 2015), and N-containing analogs of typical flavonoid – 3-O-arylmethylgalangin, active against *Hepacivirus C* reproduction (Lee et al., 2010). The potential structural candidates for the most active components in the humic molecular ensemble are shown in Table S6 in the Supplementary Material.

4. Conclusion

Assessment of anti-HIV activity and structure of two big sets of humic and shilajit materials allowed us to reveal the following trends. For the humic materials used in this study we have discovered two distinct trends in antiviral activity. The first one concerns much higher activity of the humic acids versus fulvic acids: HA > HMA > HFA > FA. The second trend concerns the source or origin: coal > peloid > peat. The both sequences follow the trend in lipophilicity index (a ratio of aromatic to aliphatic carbon) for these materials. This could be indicative of the leading role of the aromatic structures of HS in interaction with HIV. This assumption corroborates well the results of correlation analysis of the obtained EC50 values and structural composition: the closest relationships were observed for C_{ar} (−0.82) and CH_2O (+0.7). This indicates an increase in antiviral activity along with an increase in aromaticity of HS and a decrease along with a contribution of carbohydrate moieties. The obtained results are consistent with our previous

Table 2

Examples of ChEMBL compounds with anti-HIV activity corresponding to the FTICR MS formulae found in the humic materials used in this study.

| Formula	Structure	EC$_{50}$, μM	assay description	Ref.
$C_{24}H_{28}O_6$		1.3	Inhibition of HIV-1 induced CPE in CEM-SS cells	Kashman et al. (1993)
$C_{22}H_{14}N_2O_7$		0.1	Inhibition of HIV-1 induced CPE in a cell-based assay	Yeo et al. (2005)
$C_{27}H_{21}NO_{10}$		12.5	Inhibition of HIV-1 integrase by electrochemiluminescent-based high-throughput strand transfer assay	Marchand et al. (2008)
		10.1	Inhibition of HIV-1 RNase H by FRET high-throughput assay	Marchand et al. (2008)
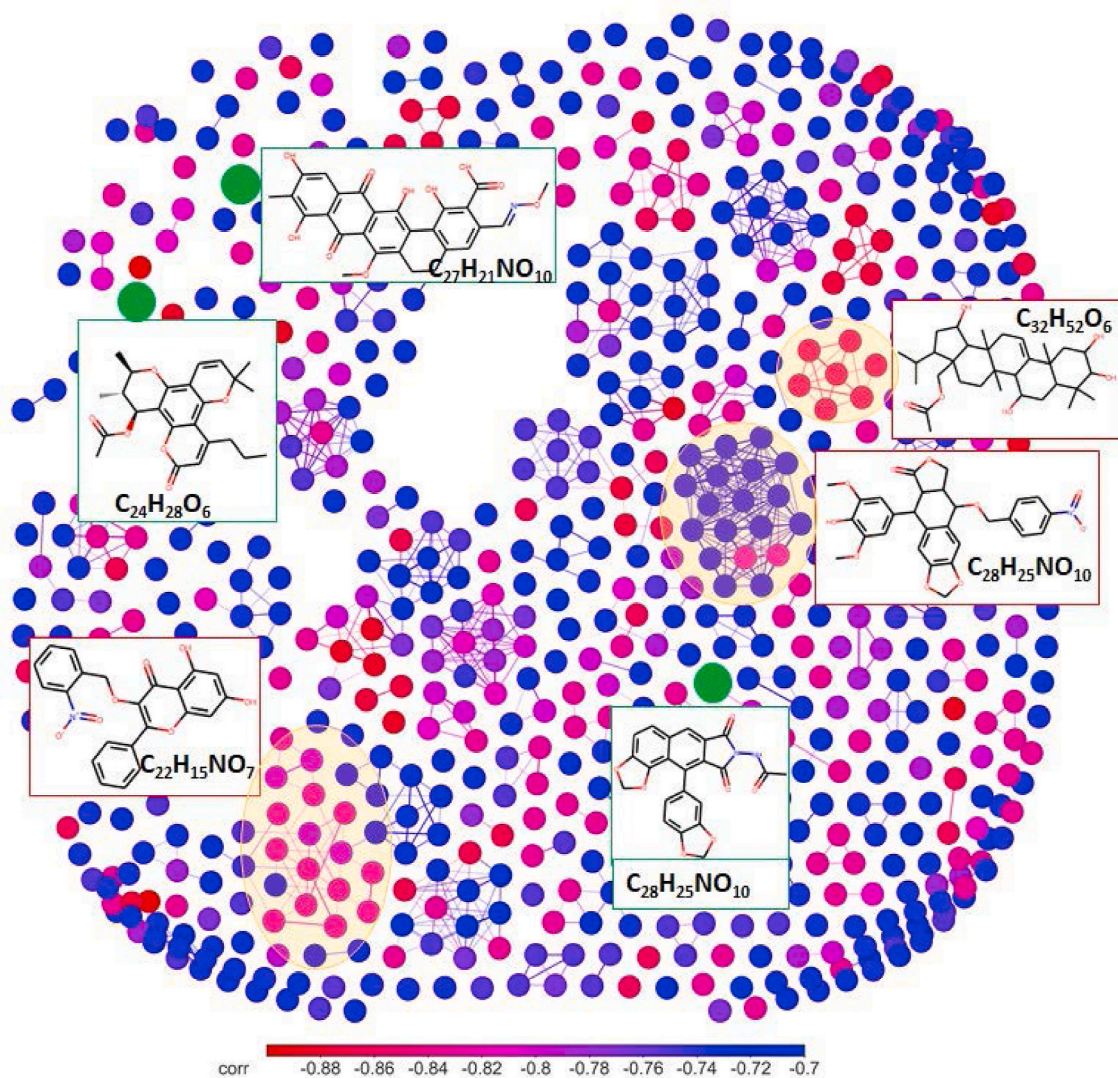
Fig. 7. Network-based representation of ChEMBL chemical space corresponding to the fomulae found in the HS samples, which were highly correlated (Spearman's rank correlation ≤ -0.7) with EC50. A network node represents chemical structure and it is labeled with the corresponding formula. An edge is drawn between a pair of nodes if the Tanimoto similarity index value was not lower than 0.8. Nodes and edges are colored by Spearman's rank correlation value. Structures presented in Table 2 are shown in green. Clusters of structures discussed in the text are highlighted by orange and their representative structures are shown. (For interpretation of the references to color in this figure legend, the reader is referred to the Web version of this article.)

findings (Zhernov et al., 2017). The low anti-HIV activity and inverse structural trends found for the shilajit samples point out to different mode of action of shilajit materials as compared to humic substances. This is consistent with very different structural and molecular composition of shilajit as compared to humic materials.

Given the data of our reported investigations (Zhernov et al., 2017), we might suggest that the hydrophobic humic materials prevent fusion and inhibit reverse transcriptase activity of HIV-1, as it was experimentally evidenced in attachment and reverse transcriptase inhibition (RTI) assays conducted in our previous studies. These studies showed that humic materials inhibited HIV-1 reverse transcriptase in a dose-dependent manner similar to AZT. The obtained values of RTI activities of HMA and HA were well within the range determined for the mixtures of different natural lignans. We obtained the similar results in the mechanistic studies using the time-of-addition (TOA) assay with the reference inhibitors: the fusion inhibitor T-20, the reverse transcription inhibitor AZT, and the integrase inhibitor RAL (Zhernov et al., 2017). The studied hydrophobic humic materials lost 50% of their efficacy at 7–8 h post-infection (h.p.i.), which is very close to AZT (7.7 ± 0.2). This also indirectly confirms the presence of RTI-activity in hydrophobic humic materials. With regard to shilajit, we might suggest that the nitrogen-rich shilajit molecules could interfere with peptide-based attachment and act as nitrogen-fusion inhibitors. This assumption can be indirectly confirmed by the data of the same TOA assay on the nitrogen-rich peloid FA: their profile was similar to fusion inhibitor T20 with a 50% loss of efficacy reached even at 5.0 ± 0.3 h.p.i. (Zhernov et al., 2017).

In general, the obtained results demonstrate that humic materials represent a rich source of highly potent and polytargeted natural compounds which might be used for prevention and treatment of viral infections. The most promising and straightforward way of humic materials use in clinical practice can be development of anti-HIV-microbicide formulations. This would improve efficacy of prevention of HIV-1 transmission. For anti-HIV-1 therapy, humic materials may supplement the first-line treatment regimens, which so far have not included entry inhibitors. Given that humic materials can be easily produced from coal or peloids and are amenable to long-term storage at room temperature without loss of anti-HIV-1 activity, they can be used for anti-HIV-1 therapy under the resource limited settings, e.g. in the South Africa, which is strongly affected by the AIDS pandemic.

Declaration of competing interest

The authors declare that they have no known competing financial interests or personal relationships that could have appeared to influence the work reported in this paper.

Acknowledgements

Appendix A. Supplementary data

Supplementary data to this article can be found online at https://doi.org/10.1016/j.envres.2020.110312.

Contributors

YZ, EK and IP conceived and designed the study. AK, MS and IP provided the HS and shilajit samples. YZ and GK performed the anti-HIV activity assessment. AK performed the ^{13}C NMR characterization and statistical calculations. AZ, AO, and EN performed the FTICR MS and ^{13}C NMR characterization, data-mining and chemometrics of the samples. EN, EK and IP supervised the study. AK, AZ, AO, MS, GK and YZ drafted the manuscript. All authors read and approved the final manuscript.

Funding

References

Agarwal, S.P., Khanna, R., Karmarkar, R., Anwer, M.K., Khar, R.K., 2007. Shilajit: a review. Phyther. Res. 21, 401–405. https://doi.org/10.1002/ptr.2100.

Andrae-Marobela, K., Ghislain, F.W., Okatch, H., Majinda, R.R.T., 2013. Polyphenols: a diverse class of multi-target anti-HIV-1 agents. Curr. Drug Metabol. 14, 392–413. https://doi.org/10.2174/1389200211314990095.

Botes, M.E., Dekker, J., van Rensburg, C.E.J., 2002. Phase I trial with oral Oxihumate in HIV-infected patients. Drug Dev. Res. 57, 34–39. https://doi.org/10.1002/ddr.10117.

Bruccoleri, A., 2013. Positional adaptability in the design of mutation-resistant nonnucleoside HIV-1 reverse transcriptase inhibitors: a supramolecular perspective. AIDS Res. Hum. Retrovir. 29, 4–12. https://doi.org/10.1089/AID.2012.0141.

Cagno, V., Donalisio, M., Civra, A., Cagliero, C., Rubiolo, P., Lembo, D., 2015. In vitro evaluation of the antiviral properties of Shilajit and investigation of its mechanisms of action. J. Ethnopharmacol. 166, 129–134. https://doi.org/10.1016/j.jep.2015.03.019.

Daglia, M., 2012. Polyphenols as antimicrobial agents. Curr. Opin. Biotechnol. 23, 174–181. https://doi.org/10.1016/j.copbio.2011.08.007.

Dong, E., Du, H., Gardner, L., 2020. An interactive web-based dashboard to track COVID-19 in real time. Lancet Infect. Dis. 20, 533–534. https://doi.org/10.1016/S1473-3099(20)30120-1.

Dong, G., Peng, C., Luo, J., Wang, C., Han, L., Wu, B., Ji, G., He, H., 2015. Adamantane-resistant influenza a viruses in the world (1902-2013): frequency and distribution of M2 gene mutations. PloS One 10, e0119115. https://doi.org/10.1371/journal.pone.0119115.

Fedoros, E.I., Orlov, A.A., Zherebker, A., Gubareva, E.A., Maydin, M.A., Konstantinov, A. I., Krasnov, K.A., Karapetian, R.N., Izotova, E.I., Pigarev, S.E., Panchenko, A.V., Tyndyk, M.L., Osolodkin, D.I., Nikolaev, E.N., Perminova, I., Anisimov, V.N., 2018. Novel water-soluble lignin derivative BP-Cx-1: identification of components and screening of potential targets in silico and in vitro. Oncotarget 9, 18578–18593. https://doi.org/10.18632/oncotarget.24990.

Ford, N., Vitoria, M., Rangaraj, A., Norris, S.L., Calmy, A., Doherty, M., 2020. Systematic review of the efficacy and safety of antiretroviral drugs against SARS, MERS or COVID-19: initial assessment. J. Int. AIDS Soc. 23, e25489 https://doi.org/10.1002/jia2.25489.

Helbig, B., Klöcking, R., Wutzler, P., 1997. Anti-herpes simplex virus type 1 activity of humic acid-like polymers and their o-diphenolic starting compounds. Antivir. Chem. Chemother. 8, 265–273. https://doi.org/10.1177/095632029700800310.

Hertkorn, N., Permin, A., Perminova, I., Kovalevskii, D., Yudov, M., Petrosyan, V., Kettrup, A., 2002. Comparative analysis of partial structures of a peat humic and fulvic acid using one- and two-dimensional nuclear magnetic resonance spectroscopy. J. Environ. Qual. 31, 375–387. https://doi.org/10.2134/jeq2002.3750.

Jeeninga, R.E., Keulen, W., Boucher, C., Sanders, R.W., Berkhout, B., 2001. Evolution of AZT resistance in HIV-1: the 41-70 intermediate that is not observed in Vivo has a replication defect. Virology 283, 294–305. https://doi.org/10.1006/viro.2001.0888.

Jooné, G.K., Dekker, J., Van Rensburg, C.E.J., 2003. Investigation of the immunostimulatory properties of oxihumate. Zeitschrift fur Naturforsch. - Sect. C J. Biosci. 58, 263–267. https://doi.org/10.1515/znc-2003-3-421.

Karamov, E., Epremyan, K., Siniavin, A., Zhernov, Y., Cuevas, M.T., Delgado, E., Sánchez-Martínez, M., Carrera, C., Kornilaeva, G., Turgiev, A., Bacqué, J., Pérez-Álvarez, L., Thomson, M.M., 2018. HIV-1 genetic diversity in recently diagnosed infections in Moscow: predominance of A FSU , frequent branching in clusters, and circulation of the Iberian subtype G variant. AIDS Res. Hum. Retrovir. 34, 629–634. https://doi.org/10.1089/aid.2018.0055.

Kashman, Y., Gustafson, K.R., Fuller, R.W., Cardellina, J.H., McMahon, J.B., Currens, M. J., Buckheit, R.W., Hughes, S.H., Cragg, G.M., Boyd, M.R., 1993. HIV inhibitory natural products. Part 7. The calanolides, a novel HIV-inhibitory class of coumarin derivatives from the tropical rainforest tree, Calophyllum lanigerum. [Erratum to document cited in CA117(11):108101g]. J. Med. Chem. 36, 1110. https://doi.org/10.1021/jm00060a020.

Khanna, R., Witt, M., Anwer, M., Agarwal, S.P., Koch, B.P., 2008. Spectroscopic characterization of fulvic acids extracted from the rock exudate Shilajit. Org. Geochem. 39, 1719–1724.

Klöcking, R., Helbig, B., Schötz, G., Schacke, M., Wutzler, P., 2002. Anti-HSV-1 activity of synthetic humic acid-like polymers derived from p-diphenolic starting com-

pounds. Antivir. Chem. Chemother. 13, 241–249. https://doi.org/10.1177/095632020201300405.

Klöcking, R., Sprössig, M., 1972. Antiviral properties of humic acids. Experientia 28, 607–608. https://doi.org/10.1007/BF01931906.

Koch, B.P., Dittmar, T., 2006. From mass to structure: an aromaticity index for high-resolution mass data of natural organic matter. Rapid Commun. Mass Spectrom. 20, 926–932. https://doi.org/10.1002/rcm.2386.

Koch, B.P., Dittmar, T., 2016. Erratum. From mass to structure: an aromaticity index for high-resolution mass data of natural organic matter. Rapid Commun. Mass Spectrom. 30 https://doi.org/10.1002/rcm.7433, 250-250.

Konstantinov, A.I., Vladimirov, G.N., Grigoryev, A.S., Kudryavtsev, A.V., Perminova, I. V., Nikolaev, E.N., 2013. Molecular composition study of Mumijo from different geographic areas using size-exclusion chromatography, NMR spectroscopy, and high-resolution mass spectrometry. In: Xu, J., Wu, J., He, Y. (Eds.), Functions of Natural Organic Matter in Changing Environment. Springer, Dordrecht, pp. 283–287. https://doi.org/10.1007/978-94-007-5634-2_52.

Kornilaeva, G.V., Siniavin, A.E., Schultz, A., Germann, A., Moog, C., von Briesen, H., Turgiev, A.S., Karamov, E.V., 2019. The differential anti-HIV effect of a new humic substance-derived preparation in diverse cells of the immune system. Acta Naturae 11, 68–76. https://doi.org/10.32607/20758251-2019-11-2-68-76.

Kovalevskii, D.V., Permin, A.B., Perminova, I.V., Petrosyan, V.S., 2000. Recovery of conditions for quantitative measuring the PMR spectra of humic acids. Moscow Univ. Chem. Bull. 41, 39–42.

Kunenkov, E.V., Kononikhin, A.S., Perminova, I.V., Hertkorn, N., Gaspar, A., Schmitt-Kopplin, P., Popov, I.A., Garmash, A.V., Nikolaev, E.N., 2009. Total mass difference statistics algorithm: a new approach to identification of high-mass building blocks in electrospray ionization fourier transform ion cyclotron mass spectrometry data of natural organic matter. Anal. Chem. 81, 10106–10115. https://doi.org/10.1021/ac901476u.

Lee, H.S., Park, K.S., Lee, B., Kim, D.E., Chong, Y., 2010. 3-O-arylmethylgalangin, a novel isostere for anti-HCV 1,3-diketoacids (DKAs). Bioorg. Med. Chem. 18, 7331–7337. https://doi.org/10.1016/j.bmc.2010.09.021.

Leefmann, T., Frickenhaus, S., Koch, B.P., 2019. UltraMassExplorer: a browser-based application for the evaluation of high-resolution mass spectrometric data. Rapid Commun. Mass Spectrom. 33, 193–202. https://doi.org/10.1002/rcm.8315.

Leydet, A., Moullet, C., Roque, J.P., Witvrouw, M., Pannecouque, C., Andrei, G., Snoeck, R., Neyts, J., Schols, D., De Clercq, E.J., 1998. Polyanion inhibitors of HIV and other viruses. 7. Polyanionic compounds and polyzwitterionic compounds derived from cyclodextrins as inhibitors of HIV transmission. J. Med. Chem. 41, 4927–4932. https://doi.org/10.1021/jm970661f.

Li, G., De Clercq, E., 2020. Therapeutic options for the 2019 novel coronavirus (2019-nCoV). Nat. Rev. Drug Discov. 19, 149–150. https://doi.org/10.1038/d41573-020-00016-0.

Lu, F.J., Tseng, S.N., Li, M.L., Shih, S.R., 2002. In vitro anti-influenza virus activity of synthetic humate analogues derived from protocatechuic acid. Arch. Virol. 147, 273–284. https://doi.org/10.1007/s705-002-8319-5.

Mai, Z.P., Zhou, K., Ge, G.B., Wang, C., Huo, X.K., Dong, P.P., Deng, S., Zhang, B.J., Zhang, H.L., Huang, S.S., Ma, X.C., 2015. Protostane triterpenoids from the Rhizome of Alisma orientale exhibit inhibitory effects on human Carboxylesterase 2. J. Nat. Prod. 78, 2372–2380. https://doi.org/10.1021/acs.jnatprod.5b00321.

Marchand, C., Beutler, J.A., Wamiru, A., Budihas, S., Möllmann, U., Heinisch, L., Mellors, J.W., Le Grice, S.F., Pommier, J., 2008. Madurahydroxylactone derivatives as dual inhibitors of human immunodeficiency virus type 1 integrase and RNase H. Antimicrob. Agents Chemother. 52, 361–364. https://doi.org/10.1128/AAC.00883-07.

Moskaleychik, F.F., Laga, V.Y., Delgado, E., Vega, Y., Fernandez-Garcia, A., Perez-Alvarez, Kornilaeva, G.V., Pronin, A.Y., Zhernov, Y.V., Thomson, M.M., Bobkova, M. R., Karamov, E.V., 2015. Rapid spread of the HIV-1 circular recombinant CRF02-AG in Russia and neighboring countries. Vopr. Virusol. 60, 14–19.

Mosmann, T., 1983. Rapid colorimetric assay for cellular growth and survival: application to proliferation and cytotoxicity assays. J. Immunol. Methods 65, 55–63. https://doi.org/10.1016/0022-1759(83)90303-4.

Nikolaev, E.N., Boldin, I.A., Jertz, R., Baykut, G., 2011. Initial experimental characterization of a new ultra-high resolution FTICR cell with dynamic harmonization. J. Am. Soc. Mass Spectrom. 22, 1125–1133. https://doi.org/10.1007/s13361-011-0125-9.

Orlov, A.A., Zherebker, A., Eletskaya, A.A., Chernikov, V.S., Kozlovskaya, L.I., Zhernov, Y.V., Kostyukevich, Y., Palyulin, V.A., Nikolaev, E.N., Osolodkin, D.I., Perminova, I.V., 2019. Examination of molecular space and feasible structures of bioactive components of humic substances by FTICR MS data mining in ChEMBL database. Sci. Rep. 9, 12066. https://doi.org/10.1038/s41598-019-48000-y.

Pottage, J.C., Kessler, H.A., 1995. Herpes simplex virus resistance to acyclovir: clinical relevance. Infect. Agents Dis. 4, 115–124.

Sander, T., Freyss, J., von Korff, M., Rufener, C., 2015. DataWarrior: an open-source program for chemistry aware data visualization and analysis. J. Chem. Inf. Model. 55, 460–473. https://doi.org/10.1021/ci500588j.

Savage, A.M., Li, Y., Matolyak, L.E., Doncel, G.F., Turner, S.R., Gandour, R.D., 2014. Anti-HIV activities of precisely defined, semirigid, carboxylated alternating copolymers. J. Med. Chem. 57, 6354–6363. https://doi.org/10.1021/jm401913w.

Schneider, J., Weis, R., Männer, C., Kary, B., Werner, A., Seubert, B.J., Riede, U.N., 1996. Inhibition of HIV-1 in cell culture by synthetic humate analogues derived from hydroquinone: mechanism of inhibition. Virology 218, 389–395. https://doi.org/10.1006/viro.1996.0208.

Schepetkin, I.A., Khlebnikov, A.I., Ah, S.Y., Woo, S.B., Jeong, C.S., Klubachuk, O.N., Kwon, B.S., 2003. Characterization and biological activities of humic substances from mumie. J. Agric. Food Chem. 51, 5245–5254. https://doi.org/10.1021/jf021101e.

Schepetkin, I.A., Xie, G., Mark, A., Jutila, M.A., Quinn, M.T., 2009. Complement-fixing activity of fulvic acid from shilajit and other natural sources. Phytother Res. 23, 373–384. https://doi.org/10.1002/ptr.2635.

Schols, D., Wutzler, P., Klöcking, R., Helbig, B., De, E.C., 1991. Selective inhibitory activity of polyhydroxycarboxylates derived from phenolic compounds against human immunodeficiency virus replication. J. Acquir. Immune Defic. Syndr. 4, 677–685.

Sleighter, R.L., Hatcher, P.G., 2007. The application of electrospray ionization coupled to ultrahigh resolution mass spectrometry for the molecular characterization of natural organic matter. J. Mass Spectrom. 42, 559–574. https://doi.org/10.1002/jms.1221.

Sleighter, R.L., Mckee, G.A., Liu, Z., Hatcher, P.G., 2008. Naturally present fatty acids as internal calibrants for fourier transform mass spectra of dissolved organic matter. Limnol Oceanogr. Methods 6, 246–253. https://doi.org/10.4319/lom.2008.6.246.

Stevenson, F., 1994. Humus Chemistry: Genesis, Composition, Reactions. Humus Chem, second ed. Wiley and Sons, New York, NY.

Van Rensburg, C.E.J., Dekker, J., Weis, R., Smith, T.L., Janse Van Rensburg, E., Schneider, J., 2002. Investigation of the anti-HIV properties of oxihumate. Chemotherapy 48, 138–143. https://doi.org/10.1159/000064919.

Wain-Hobson, S., Vartanian, J.P., Henry, M., Chenciner, N., Cheynier, R., Delassus, S., Martins, L.P., Sala, M., Nugeyre, M.T., Guétard, D., Klatzmann, D., Gluckman, J.C., Rozenbaum, W., Barré-Sinoussi, F., Montagnier, L., 1991. LAV revisited: origins of the early HIV-1 isolates from Institut Pasteur. Science 252, 961–965. https://doi.org/10.1126/science.2035026.

Yeo, H., Li, Y., Fu, L., Zhu, J.L., Gullen, E.A., Dutschman, G.E., Lee, Y., Chung, R., Huang, E.S., Austin, D.J., Cheng, Y.C., 2005. Synthesis and antiviral activity of helioxanthin analogues. J. Med. Chem. 48, 534–546. https://doi.org/10.1021/jm034265a.

Zhan, P., Pannecouque, C., De Clercq, E., Liu, X., 2016. Anti-HIV drug discovery and development: current innovations and future trends. J. Med. Chem. 59, 2849–2878. https://doi.org/10.1021/acs.jmedchem.5b00497.

Zherebker, A., Turkova, A.V., Kostyukevich, Y., Kononikhin, A., Zaitsev, K.V., Popov, I. A., Nikolaev, E., Perminova, I., 2017. Synthesis of carboxylated styrene polymer for internal calibration of Fourier transform ion cyclotron resonance mass-spectrometry of humic substances. Eur. J. Mass Spectrom. 23, 156–161. https://doi.org/10.1177/1469066717718963.

Zherebker, A.Y., Airapetyan, D., Konstantinov, A.I., Kostyukevich, Y.I., Kononikhin, A.S., Popov, I.A., Zaitsev, K.V., Nikolaev, E.N., Perminova, I.V., 2015. Synthesis of model humic substances: a mechanistic study using controllable H/D exchange and Fourier transform ion cyclotron resonance mass spectrometry. Analyst 140, 4708–4719. https://doi.org/10.1039/c5an00602c.

Zhernov, Y., 2018. Natural humic substances interfere with multiple stages of the replication cycle of human immunodeficiency virus. J. Allergy Clin. Immunol. 141, AB233. https://doi.org/10.1016/j.jaci.2017.12.737.

Zhernov, Y.V., Khaitov, M.R., 2019. Microbicides for topical immunoprevention of HIV infection (in Russ). Bull. Sib. Med. 18, 49–59. https://doi.org/10.20538/1682-0363-2019-1-49-59.

Zhernov, Y.V., Kremb, S., Helfer, M., Schindler, M., Harir, M., Mueller, C., Hertkorn, N., Avvakumova, N.P., Konstantinov, A.I., Brack-Werner, R., Schmitt-Kopplin, P., Perminova, I.V., 2017. Supramolecular combinations of humic polyanions as potent microbicides with polymodal anti-HIV-activities. New J. Chem. 41, 212–224. https://doi.org/10.1039/C6NJ00960C.

Zhou, X.M., Wang, Z.Q., Chang, J.Y., Chen, H.X., Cheng, Y.C., Lee, K.H., 1991. Antitumor agents. 120. New 4-substituted benzylamine and benzyl ether derivatives of 4'-O-demethylepipodophyllotoxin as potent inhibitors of human DNA topoisomerase II. J. Med. Chem. 34, 3346–3350. https://doi.org/10.1021/jm00116a001.